Kinetics, Isotherm and Thermodynamic Studies of the Adsorption of Reactive Red 239 Dye from Aqueous Solution by Chitosan 8B

Subarna Karmaker, Farin Sintaha, Tapan Kumar Saha*

Department of Chemistry, Jahangirnagar University, Savar, Bangladesh
Email: *tksaha_ju@yahoo.com

Abstract

The adsorption of reactive red 239 (RR239) dye onto chitosan 8B was studied in aqueous solution at various pHs, initial dye concentrations, ionic strengths and temperatures, respectively. The adsorption of dye onto chitosan 8B was confirmed by diffuse reflectance electronic absorption spectra. The adsorption of RR239 onto chitosan 8B was greatly influenced by solution pHs, initial dye concentrations, ionic strengths and temperatures. The kinetics and mechanism of dye adsorption process were analyzed by pseudo first-, second-order, Elovich and intraparticle diffusion kinetic models. The adsorption kinetics of RR239 dye followed a pseudo second-order model very well. The surface sorption and intraparticle diffusion mechanisms were involved in the actual sorption process. The equilibrium isotherm data were fitted well with the Langmuir model rather than the Freundlich, Temkin and Dubinin-Radushkevich models. The maximum dye adsorption onto chitosan 8B was estimated to be 163.93 μmol/g at 45°C. The activation energy (E_a) was obtained to be 23.30 kJ/mol. The computed thermodynamic parameters such as $\Delta G^{\ddagger}$, $\Delta H^{\ddagger}$, $\Delta S^{\ddagger}$, ΔG, ΔH and ΔS confirmed that the adsorption of RR239 dye onto chitosan 8B was a spontaneous endothermic physisorption process. Desorption test was carried out in NaOH solution (pH 12.5) and the chitosan flakes could be reused.

1. Introduction

Rapid industrialization has led to increased various types of pollutants into aq-

uatic systems that have been identified as among the main causes of environmental pollution and degradation. Dyes, which are widely used in different industries, can impede light penetration into water, retard photosynthetic activity, inhibit the growth of biota and have a tendency to chelate metal ions [1]. Accordingly, the treatment of colored dye effluent streams has been attracted the attention of environmentalists, technologists, and entrepreneurs because of its socioeconomic and political dimensions. Almost one million tons of dyes are annually produced in the world, of which azo dyes, characterized by an azo bond $(R^1 - N = N - R^2)$, represent approximately 70 wt% [2]. Azo dyes are the most common synthetic colorants released to the environment by textile, paint, varnish, paper, plastic, food, pharmaceutical, and cosmetic industries. The release of azo dyes in aquatic environment is challenging not only for aesthetic reasons but also because azo dyes and their cleavage products (aromatic amines) are carcinogenic [2] [3]. Numerous technologies, such as adsorption [4] [5] [6] [7], membrane filtration [8], coagulation [9], ozonation [10], advanced chemical oxidation [11] [12], and biological processes [13], have been developed and applied worldwide for the scavenging and/or degradation of dyestuff wastewater.

The adsorption process is an efficient method for the removal of dyes from effluent due to its low initial cost, simplicity of design, ease of operation and insensitivity to toxic substances. Activated carbon is the most widely used as an adsorbent due to its large surface area, microporous structure and high adsorption capacity [14]. However, its use is limited due to its high cost. Therefore, the use of low-cost, easily obtained, high-efficiency and eco-friendly adsorbents has been investigated as an ideal alternative to the current, more expensive methods for removing dyes from wastewater [15]. A number of reports on the application of low cost adsorbents to eliminate reactive dyes from aqueous solution appeared in literatures [16]-[22]. Chitin and its partially deacetylated derivative chitosan are biocompatible and biodegradable polymers. Chitosan have large numbers of amine and hydroxyl functional groups (**Figure 1(a)**). These functional groups are very effective and promising to isolate toxic heavy metals from aqueous solution [23] [24]. The opportunity of utilizing chitosan as a biosorbent to eliminate azo dyes from aqueous solution has also been taken into significant consideration [17] [25] [26] [27] [28] [29]. However, the related reports on utilizing chitosan to remove the reactive red 239 (RR239; **Figure 1(b)**) azo dye from aqueous solution are comparatively insufficient.

The aim of this study was to examine the ability of chitosan 8B (80% deacetylated chitin) as a low cost adsorbent to separate reactive red 239 (RR239) from aqueous solution. The influences of significant aspects, such as solution pHs, initial dye concentration, ionic strengths and temperatures on RR239 adsorption onto chitosan 8B were studied in batch mode. The potential rate controlling step and adsorption mechanisms were analyzed by several kinetic equations (*i.e.*, pseudo first-, pseudo second-order equations, Elovich and intraparticle diffusion models). Freundlich, Temkin, Dubinin-Radushkevich and Langmuir adsorption

isotherms were applied to compute the adsorption equilibrium. Activation and apparent thermodynamic parameters were also evaluated.
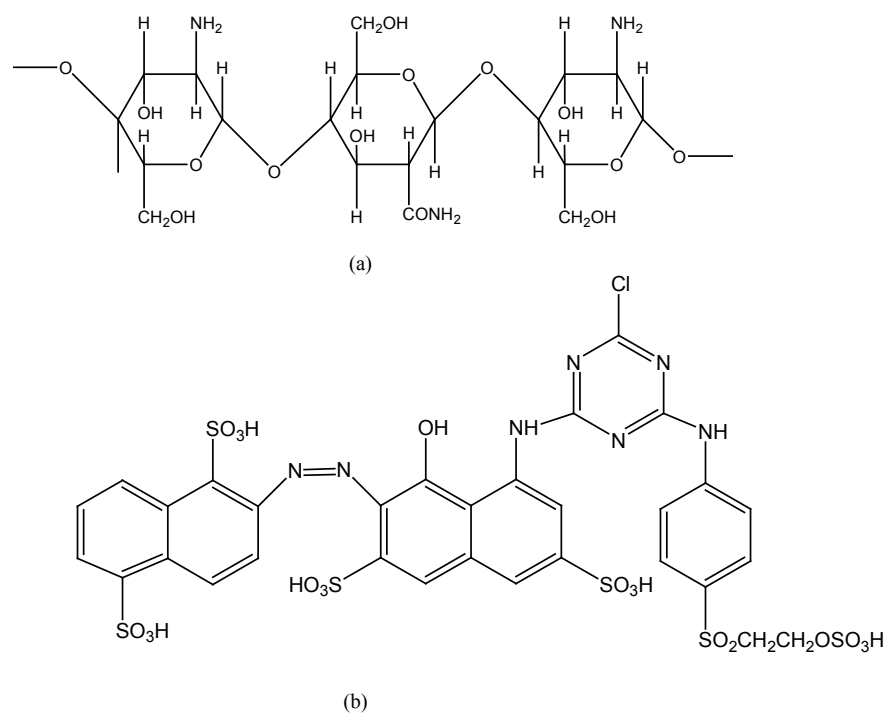
2. Experimental

2.1. Materials

Katokichi Bio Co., Ltd., Japan provided chitosan 8B (80% deacetylated chitin) which was used without further purification. A laser scattering particle size analyzer (LDSA-2400A, Tonichi Computer Applications, Japan) equipped with a dry dispersing apparatus (PD-10S, Tonichi Computer Applications, Japan) was used to determine the particle size of chitosan 8B. The mass median diameters of the chitosan 8B flakes were found to be 247 ± 9 μm.

Reactive red 239 (RR239; **Figure 1(b)**) dye was obtained from Sigma-Aldrich, Germany and was utilized without further purification. Other reagents used in the present work were analytical grade. Deionized water was prepared by circulating distilled water through a deionizing column (Barnstead, Syboron Corporation, Boston, USA).

2.2. Spectroscopic Measurements

For spectroscopic measurements, the samples were prepared by mixing solid RR239, chitosan 8B, and chitosan 8B flake-RR239 complex with solid KBr. The diffuse reflectance electronic absorption spectra of solid samples were recorded by a Varian, Cary 5000 UV-visible-NIR spectrometer (Varian Inc., USA) in the wavelength region of 200 - 800 nm.

(a)

(b)

Figure 1. The structure of (a) chitosan 8B and (b) reactive red 239 (RR239).

2.3. Batch Adsorption Experiments

Batch adsorption experiments were conducted with slight modifications of previously described method for the adsorption of reactive yellow 145 (RY145) onto chitosan in aqueous solution [26]. The adsorption of RR239 onto chitosan 8B was explored in 125 mL stoppered bottles containing a fixed amount (0.05 g) of chitosan 8B with 25 mL of dye solution (100 μmol/L). The primary pH of the dye solution was adjusted with 1 mol/L HCl or 1 mol/L NaOH solution. The pH of dye solution was measured by using a pH meter (HANNA instruments microprocessor pH meter). The stoppered bottles were shaken in a thermostated shaker at room temperature (30°C ± 0.2°C) with a speed of 120 r/min until reaching equilibrium. Each bottle was capped to avoid evaporation at high temperature. Samples were withdrawn at predetermined intervals of time for analyzing the concentration of RR239 in solution. The samples were centrifuged using a centrifuge machine (Labofuge 200, D-37520 Osterods, Germany) at a speed of 4000 rpm for 5 min. The concentration of RR239 in the supernatant was determined by spectrophotometric methods using a Shimadzu UV-1601PC spectrophotometer (Shimadzu, Japan) at λ_{max} value of 541 nm. The λ_{max} (541 nm) of RR239 solution was found to be constant at the pH ranges between 4 and 10. The apparent molar absorptivity of RR239 was estimated to be 15×10^3 L/mol/cm at 541 nm and pH 4 - 10.

The amount of RR239 adsorbed onto chitosan 8B at time t, q_t (μmol/g) was determined by

$$q_t = \frac{V(C_0 - C_t)}{m} \tag{1}$$

where C_0 (μmol/L) and C_t (μmol/L) are the liquid-phase concentrations of RR239 at initial and any time t, respectively; V(L) is the volume of RR239 solution and m (g) is the amount of dry chitosan 8B used.

The adsorption kinetics was also performed varying initial concentration of dye solutions (30 - 200 μmol/L), ionic strengths (0.01 - 0.04 mol/L) and temperatures (30°C, 35°C, 40°C and 45°C), respectively. The ionic strength of dye solutions was adjusted with 1 mol/L Na_2SO_4 solution. The equilibrium adsorption was carried out at four different temperatures (30°C, 35°C, 40°C and 45°C), and at pH 4 in absence of Na_2SO_4.

The amount of RR239 adsorbed onto chitosan 8B at equilibrium time, q_e (μmol/g) was determined by

$$q_e = \frac{V(C_0 - C_e)}{m} \tag{2}$$

where C_e (μmol/L) is the liquid-phase concentrations of RR239 at equilibrium time; C_0, V and m remain same as described above.

In the desorption study, 25 mL of 0.1 mol/L NaOH solution was used to desorb RR239 from the chitosan 8B flakes. The adsorbent was contacted with 25 mL of 100 μmol/L RR239 solution for 120 min, filtered and the adsorbent was

dried at room temperature (30˚C) overnight. The dye loaded-adsorbent was transferred into 25 mL desorbing solution and the mixture was stirred for 90 min. The amount of adsorption was determined in the same way as described above. All data presented in this paper are the mean of double measurements.

3. Results and Discussion

3.1. Spectral Studies

The chitosan 8B-RR239 complex was formulated by combining chitosan 8B flakes with a solution of RR239 at pH 4. The dye adsorption onto chitosan 8B flakes was confirmed by diffuse reflectance electronic absorption spectra. In **Figure 2**, the absorption maxima of chitosan 8B-RR239 complex were observed at around 298 and 540 nm (**Figure 2(c)**), whereas free chitosan 8B flakes exhibited two absorption peaks at 220 and 300 nm (**Figure 2(a)**), respectively. RR239 dye revealed absorption peaks at 292 and 558 nm (**Figure 2(b)**), respectively. Hence the blue shift 18 nm of the absorption peak at 540 nm, and the red shift 6 nm of the absorption peak at 298 nm must be attributed the adsorption of RR239 onto chitosan 8B flakes. However, the absorption maximum of free RR239 was found in the visible region at 541 nm in aqueous solution (pH 4 - 10).
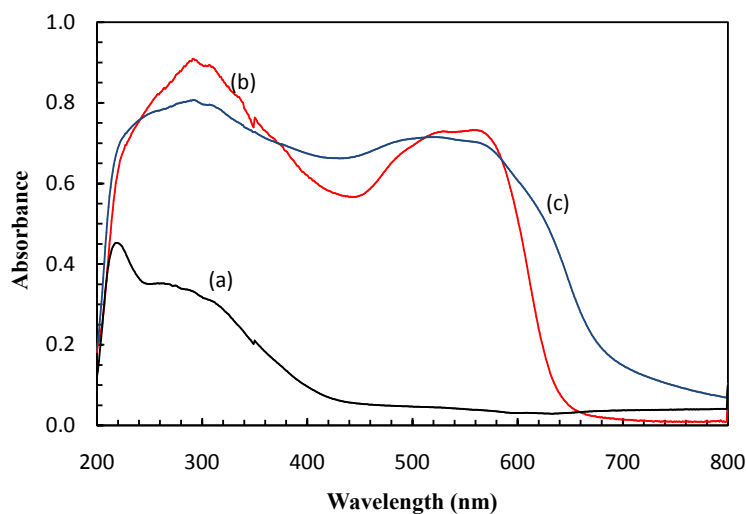
3.2. Adsorption Kinetics

3.2.1. Effect of pH on Adsorption Kinetics

The surface charge of adsorbents and the configuration of dye molecules are significantly affected by solution pH [6]. Therefore, the pH of aqueous solution is a critical issue for the period of dye adsorption process. At present study, the effect of pH on the RR239 dye adsorption capacities of chitosan 8B was conducted at varying pH (pH 4 - 10) with 100 µmol/L fixed initial dye concentrations and adsorbent dosage 0.05 g for 120 min. As can be seen from **Figure 3**, the adsorption of RR239 dye onto chitosan 8B is intimately dependent on initial pH of aqueous solution. It is noticed that the dye adsorption rate was fast for initial 10 min and subsequently it progressed at a slower rate and lastly reached equilibrium within ~60 min. However, data were received for 120 min to confirm overall equilibrium. The initial rate of dye adsorption, h (µmol/g min), decreased significantly with increasing solution pH (**Table 1**). After 120 min of sorption, the extent of equilibrium dye adsorption (q_e) was observed to be 49.70 µmol/g at pH 4 and 19.20 µmol/g at pH 10 (**Table 1**), respectively. These results can be rationalized based on the changes in surface charges of adsorbent and the structure of dye ions with changing the pH of aqueous solution. The pH_{zpc} of chitosan is 6.3. It assumes that the 99% of chitosan is protonated at pH 4.3 [26]. Hence the positively charged exteriors of chitosan 8B particles are magnificently adsorbed negatively charged dye anions in aqueous at pH 4. On the other hand, the surfaces of chitosan 8B particles turn into negative charges with rising the solution pH, causing in repulsive forces between adsorbent and anionic dye adsorbate [26],

S. Karmaker *et al.*

which ultimately causes in a smaller adsorption. The suitable solution pH was found to be 4 within the examined solution pH 4 - 10. Similar results were also observed in the adsorption of tartazine onto agricultural by-product [19] and reactive black 5 (RB5) onto chitosan [27] in aqueous solutions.

Table 1. Comparison of experimental and calculated q_e values, and kinetic parameters obtained from various kinetic models applied for the batch adsorption of RR239 dye onto chitosan 8B in aqueous solution.

Parameters	Pseudo first-order model				Pseudo second-order model				Elovich model		
	$q_{e(exp)}$ (μmol/g)	k_1 (1/min)	$q_{e(cal)}$ (μmol/g)	R^2	k_2 (g/μmol min)	$q_{e(cal)}$ (μmol/g)	h (μmol/g min)	R^2	α (μmol/g min)	β (g/μmol)	R^2
pH											
4	49.70	0.0578	15.99	0.946	0.0114	50.51	29.07	0.999	946.87	0.1890	0.953
5	43.33	0.0366	23.78	0.971	0.0043	44.64	8.67	0.999	49.86	0.1531	0.981
6	41.13	0.0389	26.41	0.995	0.0036	42.92	6.68	0.999	33.62	0.1538	0.967
7	34.13	0.0493	27.09	0.939	0.0041	35.71	5.19	0.999	29.01	0.1890	0.986
8	33.27	0.0379	23.21	0.989	0.0035	35.21	4.34	0.999	16.25	0.1719	0.953
9	30.10	0.0417	20.41	0.991	0.0045	31.75	4.49	0.999	23.07	0.2089	0.945
10	19.20	0.0387	15.59	0.995	0.0046	20.70	1.96	0.999	5.99	0.2721	0.983
[RR239] (μmol/L)											
30	14.57	0.0603	1.23	0.676	0.1941	14.62	41.49	1.000	3.40×10^6	1.3187	0.732
50	25.03	0.0739	2.30	0.730	0.1148	25.13	72.46	1.000	2.29×10^6	0.7278	0.762
100	49.33	0.0645	18.53	0.954	0.0108	50.25	27.39	1.000	1.35×10^3	0.1998	0.963
150	59.77	0.0479	24.61	0.993	0.0062	60.98	23.09	0.999	1.17×10^3	0.1633	0.979
200	71.67	0.0419	33.16	0.995	0.0039	72.99	20.79	0.999	6.17×10^2	0.1259	0974
Ionic strength (mol/L)											
0.01	49.07	0.0606	10.74	0.929	0.0195	49.50	47.85	1.000	2.38×10^4	0.2628	0.934
0.02	48.93	0.0672	13.67	0.976	0.0171	49.50	42.02	1.000	1.08×10^4	0.2463	0.943
0.03	48.80	0.0539	12.48	0.946	0.0154	49.26	37.31	1.000	9.08×10^3	0.2445	0.953
0.04	48.67	0.0534	12.71	0.953	0.0150	49.26	36.49	1.000	8.29×10^3	0.2433	0.954
Temperatures (°C)											
30	48.97	0.0458	20.31	0.939	0.0075	49.75	18.45	1.000	3.52×10^2	0.1743	0.972
35	49.47	0.0610	20.51	0.972	0.0095	50.51	24.21	1.000	5.04×10^2	0.1764	0.957
40	49.50	0.0534	18.20	0.974	0.0097	50.25	24.57	1.000	2.44×10^3	0.2159	0.979
45	49.53	0.0619	17.03	0.941	0.0120	50.25	30.30	1.000	1.68×10^3	0.2032	0.956

Figure 2. Diffuse reflectance electronic absorption spectra of (a) chitosan 8B flakes, (b) RR239, and (c) chitosan 8B-RR239 complex in KBr.
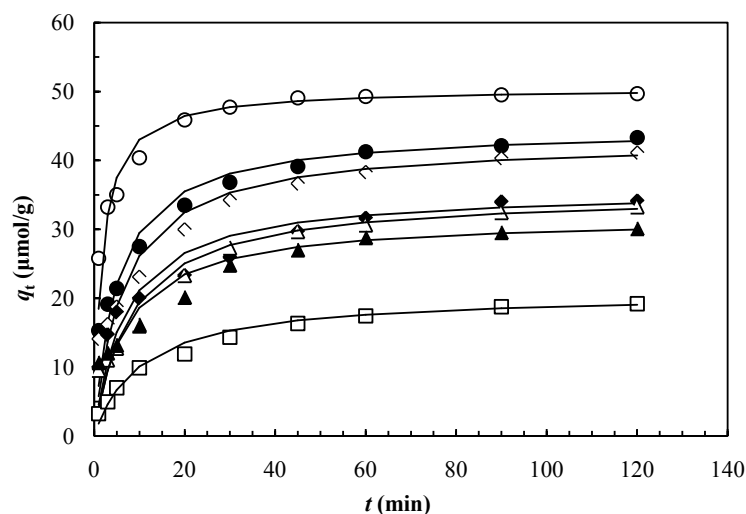
Figure 3. The effects of solution pHs on the adsorption kinetics of RR239 onto chitosan 8B in aqueous solution ([RR239]$_0$ dye: 100 µmol/L; solution volume: 25 mL; chitosan 8B: 0.05 g; temperature: 30°C ± 0.2°C; solution pHs: ○: pH 4; ●: pH 5; ◊: pH 6; ♦: pH 7; Δ: pH 8; ▲: pH 9; □: pH 10). All solid lines are numerically generated by using pseudo second-order adsorption kinetic Equation (4) and the values of $q_{e(cal)}$ and k_2 listed in Table 1.

3.2.2. Effect of Initial Dye Concentration on Adsorption Kinetics

The initial concentration supplies a significant pouring strength to overcome all mass transfer resistance of the dye between the aqueous and solid phases [21]. In this work, the influences of initial concentration of dye solutions on adsorption were studied in aqueous solution (pH 4) at 30°C for 120 min and the amount of chitosan 8B was 0.05 g. Remarkably, the amount of equilibrium RR239 dye adsorption, q_e (µmol/g), increases (**Figure 4**), but the initial rate of RR239 dye adsorption, h (µmol/g min), reduces with increasing initial dye concentration (**Table 1**), indicating that the RR239 dye adsorption onto chitosan 8B is strongly

concentration dependent. As can be seen from **Figure 4**, when the initial dye concentration increases from 30 to 200 µmol/L, the extent of dye sorption capacities of chitosan 8B increase from 14.57 to 71.67 µmol/g. These results are in accordance with obtained findings by other researchers [21] [22].

### 3.2.3. Effect of Ionic Strength on Adsorption Kinetics

The solution ionic strength is an essential issue that influences both electrostatic and non-electrostatic interactions between dyes and adsorbent surfaces. The effect of ionic strength on the adsorption kinetics of RR239 onto chitosan 8B in aqueous solution (pH 4) was successively inspected by the adding various amounts of Na$_2$SO$_4$ salt to the 100 µmol/L dye solution at 30°C. Results presented in **Figure 5** obviously showed a decrease in both the initial dye adsorption rate, h (µmol/g min), and the extent of dye adsorption, q_e (µmol/g), with increasing solution ionic strengths (**Table 1**). The results indicate that RR239 dye anions and SO$_4^{2-}$ (from Na$_2$SO$_4$) are competing for the active sorption sites, which is good agreement with previous reports [20] [26]. This also confirms the electrostatic interactions between adsorbent and dye molecules.

### 3.2.4. Effect of Temperature on Adsorption Kinetics

The kinetics of RR239 dye adsorption onto chitosan 8B was investigated in aqueous solution (pH 4) at four different temperatures, 30°C, 35°C, 40°C and 45°C and the results are depicted in **Figure 6** where the initial concentration of dye solution was 100 µmol/L. These results indicate that the initial rate of dye adsorption, h (µmol/g min), and the amount of equilibrium dye adsorption, q_e (µmol/g), increased with increasing the solution temperature (°C). Therefore,
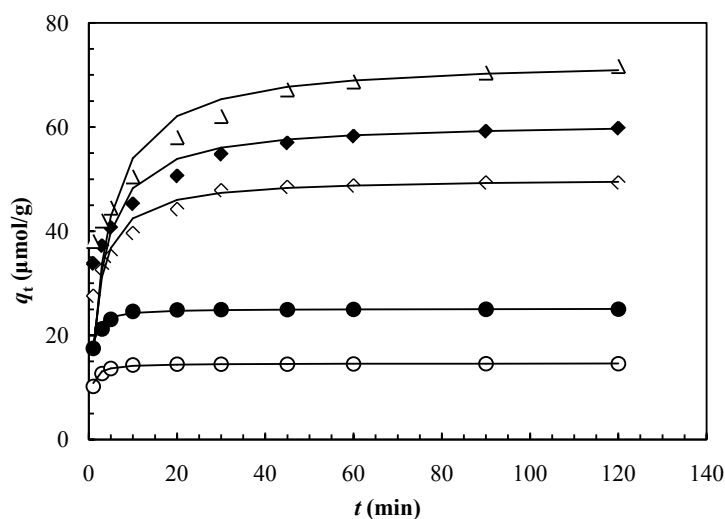
Figure 4. The effects of initial dye concentration on the adsorption kinetics of RR239 onto chitosan 8B in aqueous solution (pH 4) (solution volume: 25 mL; chitosan 8B: 0.05 g; temperature: 30°C ± 0.2°C; [RR239]$_0$: ○: 30 µmol/L; ●: 50 µmol/L; ◊: 100 µmol/L; ♦: 150 µmol/L; Δ: 200 µmol/L). All solid lines are numerically generated by using pseudo second-order adsorption kinetic Equation (4) and the values of $q_{e(cal)}$ and k_2 listed in **Table 1**.
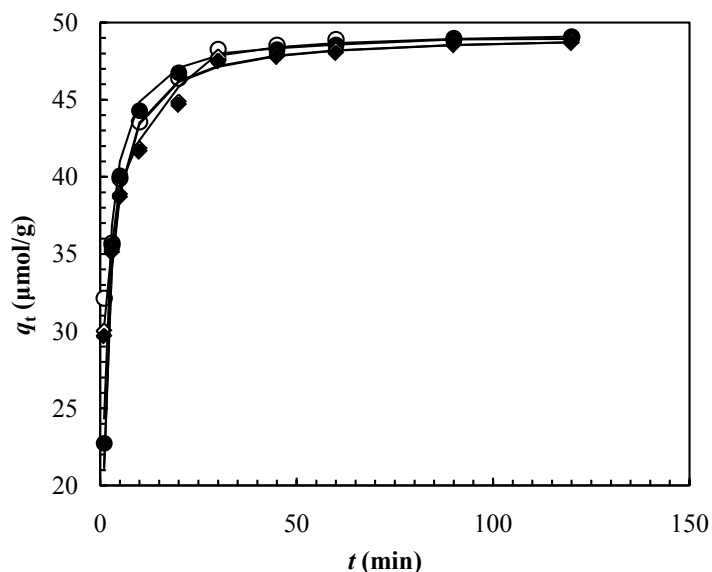
Figure 5. Adsorption kinetics of RR239 dye onto chitosan 8B in aqueous solution at various ionic strengths ([RR239]$_0$: 100 μmol/L; solution volume: 25 mL; chitosan 8B: 0.05 g; temperature: 30˚C ± 0.2˚C; ionic strength: ○: 0.01 mol/L; ●: 0.02 mol/L; ◊: 0.03 mol/L; ♦: 0.04 mol/L). All solid lines are numerically generated by using pseudo second-order adsorption kinetic Equation (4) and the values of $q_{e(cal)}$ and k_2 listed in Table 1.
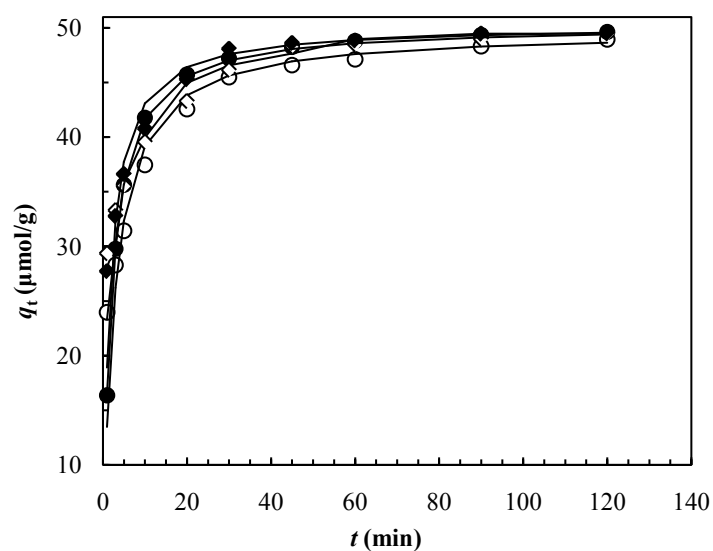
Figure 6. Adsorption kinetics of RR239 onto chitosan 8B in aqueous solution at various temperatures ([RR239]$_0$: 100 μmol/L; solution volume: 25 mL; chitosan 8B: 0.05 g; temperature: ○: 30˚C; ●: 35˚C; ◊: 40˚C; ♦: 45˚C). All solid lines are numerically generated by using pseudo second-order adsorption kinetic Equation (4) and the values of $q_{e(cal)}$ and k_2 listed in Table 1.

the RR239 dye molecules interact more efficiently with functional groups of chitosan 8B at higher temperatures because the mobility of the dye molecules increased with rising solution temperature. This is expected that rising of the solution temperature may generate a swelling effect within the internal structure of chitosan 8B [30]. Similar results were also observed in adsorption of RY145 and

RB5 onto chitosan in aqueous solutions, respectively [26] [27].

3.3. Modeling of Adsorption Kinetics

The adsorption kinetics illustrates the dye uptake rate onto the adsorbent in adsorption reaction. This is an essential feature in expressing the efficacy of adsorption. Various kinetic models have been utilized to investigate the dye adsorption mechanisms in aqueous solutions. Here, pseudo first- [31], second-order [32], Elovich [33], and intraparticle diffusion [34] kinetic models were employed to calculate the adsorption kinetic data obtained from batch experiments. The pseudo first-order adsorption kinetics is usually stated by Equation (3):

$$\log\left(q_e - q_t\right) = \log q_e - \frac{k_1}{2.0303}t \tag{3}$$

where k_1 (1/min) is the pseudo first-order sorption rate constant estimated from the slope of a plot $\log\left(q_e - q_t\right)$ versus t.

The pseudo second-order kinetic model is expressed as:

$$q_t = \frac{k_2 q_e^2 t}{1 + k_2 q_e t} \tag{4}$$

where k_2 (g/µmol min) is the pseudo second-order adsorption rate constant calculated from a linearized form of this equation, represented by Equation (5):

$$\frac{t}{q_t} = \frac{1}{k_2 q_e^2} + \frac{1}{q_e}t \tag{5}$$

The plot of t/q_t versus t would exhibit a straight line if pseudo second-order kinetics is applicable. The values of k_2 and q_e were obtained from intercept and slope of the straight line. The initial rate of adsorption, h (µmol/g min), is able to know by Equation (6):

$$h = k_2 q_e^2 \tag{6}$$

The Elovich model is generally expressed as:

$$q_t = \frac{1}{\beta}\ln\left(\alpha\beta\right) + \frac{1}{\beta}\ln t \tag{7}$$

where α (µmol/g min) is an initial rate of dye adsorption and β (g/µmol) is associated to the degree of surface coverage and the activation energy for chemisorption. The Elovich coefficients can be estimated from the plot of q_t versus $\ln t$.

The values of correlation coefficients (R^2) and kinetic parameters obtained from various applied kinetic models are presented in **Table 1**. The values of R^2 obtained from pseudo first-order (≤0.995) and Elovich (≤0.986) kinetic models are insignificant compare to the values of R^2 (≥0.999) found in the cases of pseudo second-order kinetic model. Moreover, the calculated $q_{e(cal)}$ values from pseudo second-order kinetic model and the experimental $q_{e(exp)}$ values are comparable (**Table 1**) suggesting a promising condition for pseudo second-order adsorption kinetics. Similar results were also observed in the adsorption of

RY145 and RB5 onto chitosan, respectively [26] [27].

The intraparticle diffusion model equation can be written as:

$$\text{Intraparticle diffusion model: } q_t = k_{id}t^{0.5} + I \qquad (8)$$

where k_{id} (μmol/g min$^{0.5}$) is the intraparticle diffusion rate constant and I (μmol/g) is the intercept. The typical intraparticle diffusion plots for the effect of initial dye concentration on the adsorption of RR239 onto chitosan 8B were shown in **Figure 7**. From this figure, it was observed that there were two linear portions. The intraparticle diffusion constants, k_{id1} (μmol/g min$^{0.5}$) and k_{id2} (μmol/g min$^{0.5}$), are calculated from the slope of the corresponding linear regions of **Figure 7**. The values of k_{id1} (μmol/g min$^{0.5}$) and k_{id2} (μmol/g min$^{0.5}$) express diffusion rates of the different stages in the adsorption (**Table 2**).

The changes of k_{id1} (μmol/g min$^{0.5}$) and k_{id2} (μmol/g min$^{0.5}$) represent to the adsorption levels of the exterior and interior surfaces of adsorbent [35]. The dye adsorption rate was very fast at the early stage because the RR239 was adsorbed by the exterior surface of chitosan 8B particle. When exterior surface of chitosan 8b was saturated then RR239 dye molecules entered into chitosan 8B particles and were adsorbed by the interior surface of the chitosan particles. The diffusion rate became slow. From **Figure 7**, it is also be noticed that none of the straight lines at any concentration of RR239 solution passes through the origin, which suggests that the dye adsorption mechanism was complex and both surface adsorption as well as intraparticle diffusion contributed to the actual sorption process. Similar results were also observed in the adsorption of RY145 onto chitosan in aqueous solution [26].
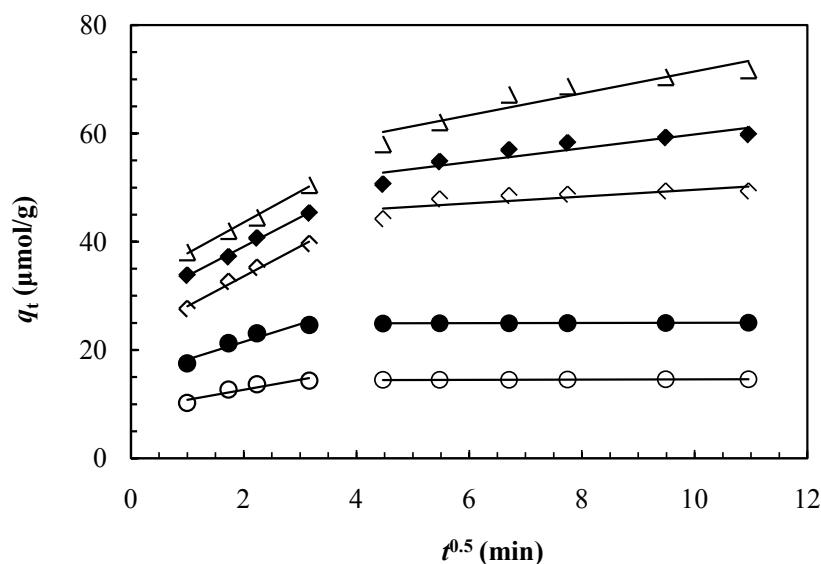
Figure 7. Typical intraparticle diffusion model plots for the adsorption of RR239 dye on Chitosan 8B at various initial concentrations (solution volume: 25 mL; chitosan 8B: 0.05 g; temperature: 30°C ± 0.2°C; initial concentrations of RR239: ○: 30 μmol/L; ●: 50 μmol/L; ◊: 100 μmol/L; ◆: 150 μmol/L; Δ: 200 μmol/L). The values of k_{id1} (μmol/g min$^{0.5}$) and k_{id2} (μmol/g min$^{0.5}$) are listed in **Table 2**.

Table 2. Diffusion rate parameters (k_{id1} and k_{id2}) for the adsorption of RR239 onto chitosan 8B in aqueous solution at various conditions.

Parameters	k_{id1} (μmol/g min$^{0.5}$)	I_1 (μmol/g)	R^2	k_{id2} (μmol/g min$^{0.5}$)	I_1 (μmol/g)	R^2
pH						
4	5.544	22.100	0.967	0.306	46.599	0.728
5	5.333	9.932	0.996	1.137	31.363	0.924
6	4.667	8.656	0.992	1.251	28.031	0.958
7	3.656	7.972	0.928	1.468	19.223	0.888
8	4.009	4.440	0.97	1.058	22.120	0.957
9	2.776	7.396	0.989	0.927	20.559	0.878
10	2.592	0.867	0.973	0.869	10.193	0.928
[RR239] (μmol/L)						
30	3.535	27.157	0.869	0.124	37.630	0.857
50	8.005	27.232	0.828	0.169	50.767	0.790
100	8.405	36.348	0.794	0.324	61.113	0.788
150	12.422	29.015	0.965	0.498	71.02	0.699
200	13.042	33.453	0.994	2.399	77.333	0.807
Ionic strength (mol/L)						
0.01	4.169	29.033	0.945	0.143	47.591	0.865
0.02	4.339	27.757	0.931	0.175	47.138	0.935
0.03	4.130	27.730	0.925	0.203	46.638	0.976
0.04	4.162	27.457	0.922	0.225	46.282	0.979
Temperatures (°C)						
30	5.449	19.013	0.989	0.628	42.233	0.987
35	6.066	19.591	0.939	0.534	44.113	0.836
40	3.991	26.162	0.983	0.519	44.106	0.787
45	4.999	24.046	0.969	0.267	46.763	0.947

3.4. Activation Parameters

The values of k_2 at various temperatures recorded in Table 1 were utilized to determine the activation energy for the adsorption of RR239 dye onto chitosan 8B in aqueous solution. According to Arrhenius equation, the rate constant (k_2), temperature (T) and activation energy (E_a) can be expressed by Equation (9):

$$\ln k_2 = -\frac{E_a}{RT} + \text{constant} \qquad (9)$$

where R (8.314 J/mol K) is the gas constant. The value of E_a was determined be 23.30 kJ/mol from the slope of straight line obtained from $\ln k_2$ versus $1/T$ plot ($R^2 = 0.928$) in temperature range 30°C - 45°C. Literature survey showed that the values of E_a were obtained to be 33.35 kJ/mol for the reactive dye adsorption on

carbon nanotubes [36], 19.72 kJ/mol for the RY145 dye adsorption onto chitosan [26] and 33.96 kJ/mol for the maxilon blue GRL dye adsorption onto sepiolite [37]. It is well known that the extent of the activation energy produces evidence on whether the adsorption is mainly physical or chemical. Wu reported that the activation energy of 5 - 40 kJ/mol is normally for physisorption process and a higher activation energy (40 - 800 kJ/mol) is for chemisorption process [36]. The value of E_a (23.30 kJ/mol) suggests that the present adsorption is a physisorption process.

The other thermodynamic activation parameters such as changes in entropy of activation ($\Delta S^{\ddagger}$), changes in enthalpy of activation ($\Delta H^{\ddagger}$), and changes in Gibbs free energy of activation ($\Delta G^{\ddagger}$), are expressed by the following relations [26]:

$$\ln\left(\frac{k_2}{T}\right) = -\frac{\Delta H^{\ddagger}}{RT} + \ln\frac{k_B}{h_P} + \frac{\Delta S^{\ddagger}}{R} \tag{10}$$

$$\Delta G^{\ddagger} = \Delta H^{\ddagger} - T\Delta S^{\ddagger} \tag{11}$$

where k_2 (g/mol min), R and T are same as described before, k_B is the Boltzman constant ($k_B = 1.381 \times 10^{-23}$ J/K) and h_P is the Plank constant ($h_P = 6.626 \times 10^{-34}$ Js). The values of $\Delta H^{\ddagger}$ and $\Delta S^{\ddagger}$ were determined from the slope and y-intercept of the straight line obtained from the plot $\ln(k_2/T)$ versus $1/T$ ($R^2 = 0.911$). The $\Delta H^{\ddagger}$ value was estimated to be 20.72 kJ/mol. The low value of $\Delta H^{\ddagger}$ shows that the interactions between RR239 and chitosan 8B are weak. The value of $\Delta S^{\ddagger}$ was determined to be −102.33 J/mol K, which indicates that the RR239 anions at activated state and at the interface are always more organized than those in the bulk solution phase [38]. Similar results were also observed in the removal of malachite green from wastewater using activated carbon and activated slag [39]. The value of $T_{av}\Delta S^{\ddagger}$ was calculated to be −31.77 kJ/mol where T_{av} represents the average value of four temperatures used for adsorption studies. The value of $\Delta H^{\ddagger}$ was found to be smaller than that of $T_{av}\Delta S^{\ddagger}$ ($\Delta H^{\ddagger} < T_{av}\Delta S^{\ddagger}$) which indicates that the impact of entropy is more significant than enthalpied in activation [38]. Moreover, the values of $\Delta G^{\ddagger}$ were found to be 51.72, 52.23, 52.75 and 53.26 kJ/mol at 30°C, 35°C, 40°C and 45°C, respectively. The positive values of $\Delta G^{\ddagger}$ suggest the existence of an energy barrier in the adsorption process [26].

3.5. Reuse of the Chitosan

The typical phenomena of RR239 dye adsorption-desorption-adsorption onto chitosan 8B flakes in aqueous are shown in **Figure 8**. In adsorption step, the initial dye concentration was 100 μmol/L with a solution pH 4.0 and a temperature 30°C whereas the release of RR239 from dye-loaded chitosan 8B was carried out in 0.1 M NaOH solution at pH 12.5 and temperature 30°C. It is observed that the amount of equilibrium dye adsorption was 49.70 μmol/g in the first adsorption step which was persisted for 120 min. The dye desorption rate was rapid for first 20 min and 85% of RR239 dye was released from dye-loaded chitosan within 35

min. After 90 min of desorption, the liberated dye from RR239-loaded chitosan was 89%. This may be due to the fact that in a basic solution, the positively charged amino groups of chitosan 8B are deprotonated, and the electrostatic interaction between chitosan and dye molecules becomes much weaker [27]. Following the desorption step, the second adsorption step took place and it repeated the similar dynamical shape of the first adsorption step. It takes 120 min to adsorb the similar amount of dye RR239 as that of desorption, and the total amount of dye adsorption is the same as that of the first adsorption step. These results show that our chitosan flakes can be reused for further dye adsorption.

3.6. Adsorption Isotherm

The analysis of the adsorption isotherm data is important to know the nature of the interaction between adsorbate and the adsorbent used for the eliminating of organic pollutants. A plot of q_e versus C_e at various temperatures is presented in Figure 9. The values of q_e increased with increasing solution temperature from 30°C to 45°C indicating that the present adsorption is an endothermic process.

The adsorption isotherm data were examined by using four isotherm models such as Ferundlich [40], Temkin [41], Dubinin-Radushkevich [42], and Langmuir [43]. Nonlinear and linear forms of all the applied models are presented as follows.

Freundlich model:

$$\text{Nonlinear form} \quad q_e = K_F C_e^{\frac{1}{n}} \tag{12}$$

$$\text{Linear form} \quad \ln q_e = \frac{1}{n}\ln C_e + \ln K_F \tag{13}$$

Temkin model:

$$\text{Nonlinear form} \quad q_e = \frac{RT}{b}\ln\left(K_T C_e\right) \tag{14}$$

$$\text{Linear form} \quad q_e = \frac{RT}{b}\ln K_T + \frac{RT}{b}\ln C_e \tag{15}$$

Dubinin-Radushkevich model:

$$\text{Nonlinear form} \quad q_e = q_{DR}\exp\left(-K_{DR}\varepsilon^2\right) \tag{16}$$

$$\text{Linear form} \quad \ln q_e = \ln q_{DR} - K_{DR}\varepsilon^2 \tag{17}$$

where $\varepsilon = RT\ln\left(1+\frac{1}{C_e}\right)$

Langmuir model:

$$\text{Nonlinear form} \quad q_e = \frac{K_L C_e}{1+a_L C_e} \tag{18}$$

$$\text{Linear form} \quad \frac{C_e}{q_e} = \frac{1}{K_L} + \frac{a_L}{K_L}C_e \tag{19}$$

where C_e (μmol/L) is the equilibrium RR239 dye concentration in solution, K_F

((μmol/g) (μmol/L)$^{-1/n}$) and n are Freundlich isotherm constants indicating the capacity and intensity of the adsorption, respectively. K_T (μmol/L) is the Temkin isotherm constant, b (J/mol) is a constant related to heat of adsorption, R (8.314 J/mol K) is an ideal gas constant and T is the absolute temperature (K). The q_e (μmol/g) is the amount of equilibrium RR239 dye adsorbed per unit weight of adsorbent, q_{DR} is the maximum adsorption capacity, K (mol^2/kJ^2) is the activity coefficient useful in obtaining the mean sorption energy E (kJ/mol) and ε is the Polanyi potential. K_L (L/g) and a_L (L/μmol) are the characteristic constants of the Langmuir equation, and the ratio of K_L/a_L gives the maximum dye adsorption capacity q_m (μmol/g) of chitosan 8B. The values of isotherm parameters are given in Table 3. In all cases, Langmuir isotherm has highest correlation coefficients (R^2), which is considerably a better fit compared with Freundlich, Temkin and Dubinin-Radushkevich adsorption isotherms.
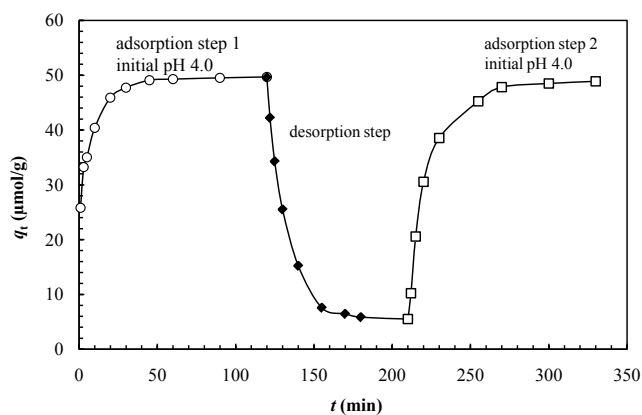
Figure 8. Adsorption and desorption kinetics of RR239 on chitosan 8B in aqueous solution at 30˚C and 100 μmol/L initial dye concentration with three steps: adsorption step 1 at initial pH 4.0, desorption step at initial pH 12.5, and adsorption step 2 at initial pH 4.0.
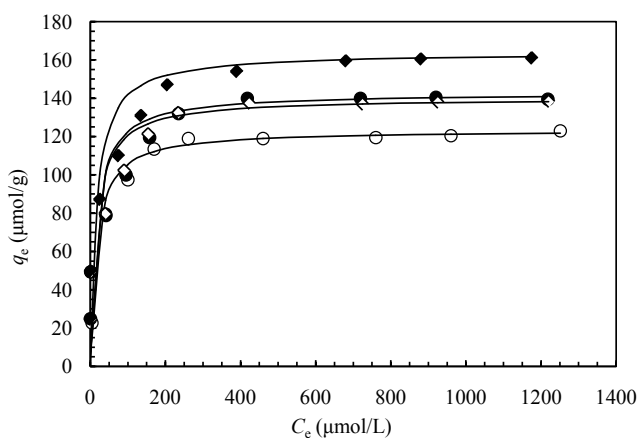
Figure 9. Adsorption isotherm of RR239 onto chitosan 8B in aqueous solution at various temperatures ([RR239]$_0$: 50 - 1500 μmol/L; solution volume: 25 mL; chitosan: 0.05 g; solution: pH 4; temperatures: ○: 30˚C; ●: 35˚C; ◊: 40˚C; ♦: 45˚C). All solid lines are numerically generated by using the Langmuir model in Equation (18) and the Langmuir isotherm constants listed in Table 3.

Table 3. Freundlich, Temkin, Dubinin-Radushkevich and Langmuir isotherm constants at different temperatures and thermodynamic parameters for the adsorption of dye RR239 onto chitosan 8B in aqueous solution at pH 4.

Parameters	Freundlich isotherm			
T (°C)	30	35	40	45
K_F ((μmol/g) (μmol/L)$^{-1/n}$)	36.885	38.425	38.502	49.824
n	5.266	4.933	4.955	5.485
R^2	0.900	0.940	0.919	0.967
Parameters	Temkin isotherm			
T (°C)	30	35	40	45
K_T (μmol/L)	24.487	14.702	14.919	64.777
b (J/mol)	201.741	171.848	175.616	182.991
R^2	0.963	0.957	0.957	0.965
Parameters	Dubinin-Radushkevich isotherm			
T (°C)	30	35	40	45
q_{DR} (μmol/g)	107.32	116.75	120.00	129.67
K (J^2/mol^2)	2.00×10^{-7}	2.00×10^{-7}	2.00×10^{-7}	3.00×10^{-7}
E (kJ/mol)	1.58	1.58	1.58	4.08
R^2	0.899	0.825	0.895	0.816
Parameters	Langmuir isotherm			
T (°C)	30	35	40	45
K_L (L/g)	7.148	8.496	8.496	10.225
a_L (L/μmol)	0.0579	0.0595	0.0603	0.0624
q_m (μmol/g)	123.46	142.86	140.85	163.93
R_L	0.0113	0.0111	0.0109	0.0106
R^2	0.999	0.999	0.999	0.999
Thermodynamic parameters				
T (°C)	30	35	40	45
ΔG (kJ/mol)	−27.63	−28.15	−28.64	−29.19
ΔH (kJ/mol)	3.80			
ΔS (J/K mol)	103.72			
R^2	0.977			

It is stated that the characteristics of the Langmuir isotherm can be expressed in terms of separation factor (R_L) [44], which is expressed in Equation (20):

$$R_L = \frac{1}{1 + a_L C_0} \tag{20}$$

where a_L (L/µmol) is the Langmuir equilibrium constant and C_0 (µmol/L) is the highest initial dye concentration. The shape of the isotherm can be interpreted as shown in **Table 4** based on the value of R_L. The values of R_L were found to be from 0 to 1 at 30°C, 35°C, 40°C and 45°C, respectively, which indicates that the adsorption is favorable at all temperatures [26].

The applicability of the Langmuir model suggests homogeneous surfaces of the chitosan 8B and monolayer coverage of RR239 dye onto the adsorbent. According to Langmuir, the maximum dye adsorption capacity of chitosan 8B was found to be 123.46 µmol/g at 30°C and 163.93 µmol/g at 45°C, respectively. This value is much higher than that of previously reported adsorbents as shown in **Table 5** [45] [46] [47].

3.7. Thermodynamics

Thermodynamic parameters related to the adsorption process, *i.e.*, Gibb's free energy change (ΔG, kJ/mol), enthalpy change (ΔH, kJ/mol), and entropy change (ΔS, J/mol K) are determined by using the values of Langmuir binding constant (a_L, L/mol) and the following equations:

$$\Delta G = -RT \ln a_L \qquad (21)$$

$$\ln a_L = \frac{\Delta S}{R} - \frac{\Delta H}{RT} \qquad (22)$$

Table 4. The relation between the value of R_L and type of adsorption.

Value of R_L	Type of adsorption
$R_L > 1.0$	Unfavorable
$R_L = 1.0$	Linear
$0 < R_L < 1.0$	Favorable
$R_L = 0$	Irreversible

Table 5. The maximum adsorption capacity (q_m) for RR239 of various adsorbents.

Adsorbents	q_m (µmol/g)	Reference
2,2'-(butane-1,4-diylbis(oxy))dibenzaldehyde cross-linked magnetic chitosan nanoparticles	176.01	[17]
Chitosan 8B	163.93	This study
Hexamethylenediamine (HMDA)-modified zeolite	25.14	[45]
Formaldehyde treated carra sawdust	13.29	[16]
Hexadecyltrimethylammonium bromide (HTAB)-modified zeolite	9.78	[46]
Hexadecyltrimethylammonium bromide (HTAB)-modified sepiolite	9.58	[46]
Cetyltrimethylammonium bromide (CTAB)-modified zeolite	8.01	[47]

where R (8.314 J/mol K) is the universal gas constant and T is the absolute temperature (K). ΔH and ΔS values can be calculated from the slope and y-intercept of the linear polt of $\ln a_L$ versus $1/T$ ($R^2 = 0.978$). The thermodynamic results are presented in Table 3. Enthalpy changes (ΔH) indicate that the present adsorption followed endothermic processes. The positive values of ΔS confirm that there was increase in the randomness at the solid-liquid interface during the adsorption of RR239 onto chitosan 8B, which results from the higher translational entropy developed by the displaced water molecules as compared to that lost as a result of dye uptake. Negative values of ΔG indicate that the RR239 dye adsorption by chitosan 8B adsorbents is a spontaneous process and more favorable process at higher temperature. The increase in the adsorption capacities of Chitosan 8B at higher temperatures may be attributed to the enhanced mobility and penetration of dye molecules within the adsorbent porous structures by overcoming the activation energy barrier and enhancing the rate of intraparticle diffusion [48].

4. Conclusion

In the present study, RR239 dye adsorption onto chitosan 8B was investigated in an aqueous solution. The effect of working parameters such as solution pHs, initial dye concentrations, ionic strengths and temperatures on the adsorption of RR239 was investigated. The obtained results suggested that all the parameters had a strong effect on the adsorption kinetics and equilibrium adsorption of RR239 onto the adsorbent. The batch adsorption kinetics was well explained by pseudo second-order model while intraparticle diffusion performed significant role in the rate limiting step. The batch adsorption kinetic profiles were absolutely reproduced by numerical analysis based on the pseudo second-order kinetic model in Equation (4) using the values of k_2 and $q_{e(cal)}$ given in Table 1. Adsorption isotherms were fitted well with the Langmuir model rather than the Freundlich, Temkin and Dubinin-Radushkevich models. The maximum RR239 dye adsorption capacity of chitosan 8B was found to be 163.93 μmol/g at 45˚C. Thermodynamic parameters showed that the RR239 dye adsorption onto chitosan 8B was spontaneous endothermic physisorption process. The significant amount (89%) of RR239 dye was released from dye-loaded chitosan in 0.1 M NaOH solution (pH 12.5) and the chitosan flakes could be reused. The present works confirm that the easily obtainable chitosan 8B can be utilized as an efficient biosorbent to remove reactive dyes from industrial wastewater.

Acknowledgements

tingen University, Germany where he has taken the diffuse reflectance electronic absorption spectra of solid samples). Authors are thankful to Prof. Yoshinobu Fukumori and Prof. Hideki Ichikawa (Kobe Gakuin University, Kobe, Japan) for providing the sample of chitosan 8B and measuring its particle size.

Conflicts of Interest

The authors declare no conflicts of interest regarding the publication of this paper.

References

[1] Ngah, W.S.W., Ariff, N.F.M., Hashim, A. and Hanafiah, M.A.K.M. (2010) Malachite Green Adsorption onto Chitosan Coated Bentonite Beads: Isotherms, Kinetics and Mechanism. *Clean—Soil*, *Air*, *Water*, **38**, 394-400. https://doi.org/10.1002/clen.200900251

[2] Saha, T.K., Frauendorf, H., John, M., Dechert, S. and Meyer, F. (2013) Efficient Oxidative Degradation of Azo Dyes by a Water-Soluble Manganese Porphyrin Catalyst. *ChemCatChem*, **5**, 796-805. https://doi.org/10.1002/cctc.201200475

[3] Weisburger, J.H. (2002) Comments on the History and Importance of Aromatic and Heterocylic Amines in Public Health. *Mutation Research*, **506-507**, 9-20. https://doi.org/10.1016/S0027-5107(02)00147-1

[4] Ali, I. and Gupta, V.K. (2006) Advances in Water Treatment by Adsorption Technology. *Nature Protocols*, **1**, 2661-2667. https://doi.org/10.1038/nprot.2006.370

[5] Ali, I. (2012) New Generation Adsorbents for Water Treatment. *Chemical Reviews*, **112**, 5073-5091. https://doi.org/10.1021/cr300133d

[6] Ai, L., Zhang, C., Liao, F., Wang, Y., Li, K., Meng, L. and Jiang, J. (2011) Removal of Methylene Blue from Aqueous Solution with Magnetite Loaded Multi-Wall Carbon Nanotube: Kinetic, Isotherm and Mechanism Analysis. *Journal of Hazardous Materials*, **198**, 282-290. https://doi.org/10.1016/j.jhazmat.2011.10.041

[7] Gomez, V., Larrechi, M.S. and Callao, M.P. (2007) Kinetic and Adsorption Study of Acid Dye Removal Using Activated Carbon. *Chemosphere*, **69**, 1151-1158. https://doi.org/10.1016/j.chemosphere.2007.03.076

[8] Thamaraiselvan, C. and Noel, M. (2015) Membrane Processes for Dye Wastewater Treatment: Recent Progress in Fouling Control. *Critical Reviews in Environmental Science and Technology*, **45**, 1007-1040. https://doi.org/10.1080/10643389.2014.900242

[9] Olad, A., Ghadim, A.R.A., Dorraji, M.S.S. and Rasoulifard, M.H. (2010) Removal of the Alphazurine FG Dye from Simulated Solution by Electrocoagulation. *Clean—Soil*, *Air*, *Water*, **38**, 401-408. https://doi.org/10.1002/clen.200900213

[10] Khadhraoui, M., Trabelsi, H., Ksibi, M., Bouguerra, S. and Elleuch, B. (2009) Discoloration and Detoxification of a Congo Red Dye Solution by Means of Ozone Treatment for a Possible Water Reuse. *Journal of Hazardous Materials*, **161**, 974-981. https://doi.org/10.1016/j.jhazmat.2008.04.060

[11] Sires, I., Guivarch, E., Oturan, N. and Oturan, M.A. (2008) Efficient Removal of Triphenylmethane Dyes from Aqueous Medium by *in Situ* Electrogenerated Fenton's Reagent at Carbon-Felt Cathode. *Chemosphere*, **72**, 592-600. https://doi.org/10.1016/j.chemosphere.2008.03.010

[12] Kim, D.S. and Park, Y.S. (2008) Comparison Study of Dyestuff Wastewater Treat-

ment by the Coupled Photocatalytic Oxidation and Biofilm Process. *Chemical Engineering Journal*, **139**, 256-263. https://doi.org/10.1016/j.cej.2007.07.095

[13] Mishra, S. and Maiti, A. (2018) The Efficacy of Bacterial Species to Decolourise Reactive Azo, Anthroquinone and Triphenylmethane Dyes from Wastewater: A Review. *Environmental Science and Pollution Research*, **25**, 8286-8314. https://doi.org/10.1007/s11356-018-1273-2

[14] Martins, T.D., Schimmel D, das Santos, J.B.O. and da Silva, E.A. (2013) Reactive Blue 5G Adsorption onto Activated Carbon: Kinetics and Equilibrium. *Journal of Chemical & Engineering Data*, **58**, 106-114. https://doi.org/10.1021/je300946j

[15] Nemr, A.E., Abdelwahab, O., EI-Sikaily, A. and Khaled, A. (2009) Removal of Direct Blue-86 from Aqueous Solution by New Activated Carbon Developed from Orange Peel. *Journal of Hazardous Materials*, **161**, 102-110. https://doi.org/10.1016/j.jhazmat.2008.03.060

[16] Sanchez, N., Benedetti, T.M., Vazquez, M., de Torresi, S.I.C. and Torresi, R.M. (2012) Kinetic and Thermodynamic Studies on the Adsorption of Reactive Red 239 by Carra Sawdust Treated with Formaldehyde. *Adsorption Science & Technology*, **30**, 881-899. https://doi.org/10.1260/0263-6174.30.10.881

[17] Banaei, A., Yaychi, M.F., Karimi, S., Vojoudi, H., Namazi, H., Badiei, A. and Pourbasheer, E. (2018) 2,2'-(Butane-1,4-diylbis(oxy))dibenzaldehyde Cross-Linked Magnetic Chitosan Nanoparticles as a New Adsorbent for the Removal of Reactive Red 239 from Aqueous Solutions. *Materials Chemistry and Physics*, **212**, 1-11. https://doi.org/10.1016/j.matchemphys.2018.02.036

[18] Caglar, E., Donari, Y.O., Sinag, A., Birogul, I., Bilge, S., Aydincak, K. and Pliekhov, O. (2018) Adsorption of Anionic and Cationic Dyes on Biochars, Produced by Hydrothermal Carbonization of Waste Biomass: Effect of Surface Functionalization and Ionic Strength. *Turkish Journal of Chemistry*, **42**, 86-99. https://doi.org/10.3906/kim-1704-12

[19] Banerjee, S. and Chattopadhyaya, M.C. (2017) Adsorption Characteristics for the Removal of a Toxic Dye Tartazine from Aqueous Solutions by a Low Cost Agricultural By-Product. *Arabian Journal of Chemistry*, **10**, S1629-S1638. https://doi.org/10.1016/j.arabjc.2013.06.005

[20] Karmaker, S., Uddin, M.N., Ichikawa, H., Fukumori, Y. and Saha, T.K. (2015) Adsorption of Reactive Orange 13 onto Jackfruit Seed Flakes in Aqueous Solution. *Journal of Environmental Chemical Engineering*, **3**, 583-592. https://doi.org/10.1016/j.jece.2014.09.010

[21] Bazrafshan, E., Mostafapour, F.K., Hosseini, A.R., Khorshid, A.R. and Mahvi, A.H. (2013) Decolorisation of Reactive Red 120 Dye by Using Single-Walled Carbon Nanotubes in Aqueous Solutions. *Journal of Chemistry*, **2013**, Article ID: 938374. doi: http://dx.doi.org/10.1155/2013/938374

[22] Shirmardi, M., Mesdaghinia, A.R., Mahvi, A.H., Nasseri, S. and Nabizadeh, R. (2012) Kinetics and Equilibrium Studies on Adsorption of Acid Red 18 (Azo-Dye) Using Multiwall Carbon Nanotubes (MWCNTs) from Aqueous Solution. *E-Journal of Chemistry*, **9**, 2371-2383. https://doi.org/10.1155/2012/541909

[23] Ngaha, W.S.W., Teonga, L.C. and Hanafiaha, M.A.K.M. (2011) Adsorption of Dyes and Heavy Metal Ions by Chitosan Composites: A Review. *Carbohydrate Polymers*, **83**, 1446-1456. https://doi.org/10.1016/j.carbpol.2010.11.004

[24] Wu, F.C., Tseng, R.L. and Juang, R.S. (2010) A Review and Experimental Verification of Using Chitosan and Its Derivatives as Adsorbents for Selected Heavy Metals. *Journal of Environmental Management*, **91**, 798-806.

https://doi.org/10.1016/j.jenvman.2009.10.018

[25] Chiou, M.S. and Li, H.Y. (2003) Adsorption Behavior of Reactive Dye in Aqueous Solution on Chemical Crosslinked Chitosan Beads. *Chemosphere*, **50**, 1095-1105. https://doi.org/10.1016/S0045-6535(02)00636-7

[26] Karmaker, S., Sen, T. and Saha, T.K. (2015) Adsorption of Reactive Yellow 145 onto Chitosan in Aqueous Solution: Kinetic Modeling and Thermodynamic Analysis. *Polymer Bulletin*, **72**, 1879-1897. https://doi.org/10.1007/s00289-015-1378-4

[27] Saha, T.K., Bhoumik, N.C., Karmaker, S., Ahmed, M.G., Ichikawa, H. and Fukumori, Y. (2011) Adsorption Characteristics of Reactive Black 5 from Aqueous Solution onto Chitosan. *Clean—Soil*, *Air*, *Water*, **39**, 984-993. https://doi.org/10.1002/clen.201000315

[28] Chiou, M.S. and Li, H.Y. (2002) Equilibrium and Kinetic Modeling of Adsorption of Reactive Dye on Cross-Linked Chitosan Beads. *Journal of Hazardous Materials*, **93**, 233-248. https://doi.org/10.1016/S0304-3894(02)00030-4

[29] Hasan, M., Ahmad, A.L. and Hameed, B.H. (2008) Adsorption of Reactive Dye onto Cross-Linked Chitosan/Oil Palm Ash Composite Beads. *Chemical Engineering Journal*, **136**, 164-172. https://doi.org/10.1016/j.cej.2007.03.038

[30] Bhattacharyya, K.G. and Sharma, A. (2003) Adsorption Characteristics of the Dye, Brilliant Green, on Neem Leaf Powder. *Dyes and Pigments*, **57**, 211-222. https://doi.org/10.1016/S0143-7208(03)00009-3

[31] Lagergren, S.Y. (1898) Zur theorie der sogenannten adsorption geloster stoffe. Kungliga Svenska Vetenskapsakad, Stockholm, **24**, 1-39.

[32] McKay, G. and Ho, Y.S. (1999) Pseudo-Second Order Model for Sorption Processes. *Process Biochemistry*, **34**, 451-465. https://doi.org/10.1016/S0032-9592(98)00112-5

[33] Elovich, S.Y. and Larinov, O.G. (1962) Theory of Adsorption from Solutions of Non Electrolytes on Solid (I) Equation Adsorption from Solutions and the Analysis of Its Simplest Form, (II) Verification of the Equation of Adsorption Isotherm from Solutions. *Otdelenie Khimicheskikh Nauk*, **2**, 209-216.

[34] Weber, W.J. and Morris, J.C. (1963) Kinetics of Adsorption on Carbon from Solution. *American Society of Civil Engineers*, **89**, 31-60.

[35] Eren, E., Cubuk, O., Ciftci, H., Eren, B. and Caglar, B. (2010) Adsorption of Basic Dye from Aqueous Solutions by Modified Sepiolite: Equilibrium, Kinetics and Thermodynamics Study. *Desalination*, **252**, 88-96. https://doi.org/10.1016/j.desal.2009.10.020

[36] Wu, C.H. (2007) Adsorption of Reactive Dye onto Carbon Nanotubes: Equilibrium, Kinetics and Thermodynamics. *Journal of Hazardous Materials*, **144**, 93-100. https://doi.org/10.1016/j.jhazmat.2006.09.083

[37] Dogan, M., Alkan, M., Demirbas, O., Ozdemir, Y. and Ozmetin, C. (2006) Adsorption Kinetics of Maxilon Blue GRL onto Sepiolite from Aqueous Solutions. *Chemical Engineering Journal*, **124**, 89-101. https://doi.org/10.1016/j.cej.2006.08.016

[38] Eren, E. (2010) Adsorption Performance and Mechanism in Binding of Azo Dye by Raw Bentonite. *Clean—Soil*, *Air*, *Water*, **38**, 758-763. https://doi.org/10.1002/clen.201000060

[39] Gupta, K.V., Srivastava, S.K. and Mohan, D. (1997) Equilibrium Uptake, Sorption Dynamics, Process Optimization and Column Operation for the Removal and Recovery of Malachine Green from Wastewater Using Activated Carbon and Activated Slag. *Industrial & Engineering Chemistry Research*, **36**, 2207-2218. https://doi.org/10.1021/ie960442c

[40] Freundlich, H. (1906) Adsorption Solution. *Zeitschrift für Physikalische Chemie*,

57, 384-470.

[41] Temkin, M.I. and Pyzhev, V. (1940) Kinetics of Ammonia Synthesis on Promoted Iron Catalyst. *Acta Physicochimica URSS*, **12**, 327-356.

[42] Inyinbor, A.A., Adekola, F.A. and Olatunji, G.A. (2016) Kinetics, Isotherms and Thermodynamic Modeling of Liquid Phase Adsorption of Rhodamine B Dye onto *Raphia hookerie* Fruit Epicarp. *Water Resources and Industry*, **15**, 14-27. https://doi.org/10.1016/j.wri.2016.06.001

[43] Langmuir, I. (1918) Adsorption of Gases on Plain Surfaces of Glass Mica Platinum. *Journal of the American Chemical Society*, **40**, 1361-1403. https://doi.org/10.1021/ja02242a004

[44] Hall, K.R., Eagleton, L.C., Acrivers, A. and Vermenlem, T. (1966) Pore- and Solid-Diffusion Kinetics in Fixed-Bed Adsorption under Constant Pattern Conditions. *Industrial & Engineering Chemistry Fundamentals*, **5**, 212-223. https://doi.org/10.1021/i160018a011

[45] Alver, E. and Metin, A.Ü. (2012) Anionic Dye Removal from Aqueous Solution Using Modified Zeolite: Adsorption Kinetics and Isotherm Studies. *Chemical Engineering Journal*, **200-202**, 59-67. https://doi.org/10.1016/j.cej.2012.06.038

[46] Ozdemir, O., Armagan, B., Turan, M. and Celik, M.S. (2004) Comparison of the Adsorption Characteristics of Azo-Reactive Dyes on Mezoporous Minerals. *Dyes and Pigments*, **62**, 49-60. https://doi.org/10.1016/j.dyepig.2003.11.007

[47] Karadag, D., Turan, M., Akgul, E., Tok, S. and Faki, A. (2007) Adsorption Equilibrium and Kinetics of Reactive Black 5 and Reactive Red 239 in Aqueous Solution onto Surfactant-Modified Zeolite. *Journal of Chemical & Engineering Data*, **52**, 1615-1620. https://doi.org/10.1021/je7000057

[48] Calvete, T., Lima, E.C., Cardoso, N.F., Dias, S.L.P. and Ribeiro, E.S. (2010) Removal of Brilliant Green Dye from Aqueous Solutions Using Homemade Activated Carbons. *Clean—Soil, Air, Water*, **38**, 521-532. https://doi.org/10.1002/clen.201000027